Hindawi
Journal of Nanomaterials
Volume 2020, Article ID 4536165, 7 pages
https://doi.org/10.1155/2020/4536165

Research Article

Prediction for the Flexural Properties of Nanowires in Lateral Manipulation

Lin Fang,[1] Quan Yuan ,[2] and Mengyang Huang[2]

[1]*China Merchants Chongqing Communications Research & Design Institute Co., Ltd, Chongqing 400067, China*
[2]*School of Civil Engineering, Architecture and Environment, Xihua University, Hongguang Town, Chengdu 610039, China*

Correspondence should be addressed to Quan Yuan; yuanqxh@163.com

Received 24 July 2019; Revised 10 November 2019; Accepted 9 December 2019; Published 3 January 2020

Academic Editor: Kishore Sridharan

Simple beam theory is usually employed to predict the flexural properties of nanowires (NWs) in the lateral manipulation, which results in a linear $F-\delta$ curve. However, three factors, namely, changes in the load position and direction of the AFM tip, surface effects, and the large displacement of the NW, are not considered in simple beam theory. In this work, a simple geometrical model is proposed to analyze the large deflection and rotational angle deformation of NWs in the lateral manipulation. The traditional solution to the differential equation of the deflection curve turns the solution of an integral equation. Results show that contact force does not linearly increase with increasing displacement, and the $F-\delta$ curve exists a maximum amount due to changes in the load position and direction of the AFM tip. Moreover, the rotational angle and deflection have a nonlinear relationship. Comparison of the results of this work with other authors' measurements illustrates that the use of simple beam theory in manipulation underestimates the deflection and effective modulus of NWs. Our model provides a good approach to predict $F-\delta$ curves, rotational angles, and contact forces that closely match experimental results.

1. Introduction

Optical manipulation has been widely used to measure the elasticity, strength, and toughness of nanomaterials [1–6]. Nanomanipulation processes can be broadly classified into three types: (1) lateral noncontact, (2) tapping mode, and (3) lateral contact [7]. The lateral noncontact nanomanipulation combined with a Scanning Tunneling Microscope (STM) or an Atomic Force Microscope (AFM) is mainly applied for bioobject in liquid. The tapping mode AFM reduces sample destruction and is widely used for studying compliant materials such as polymers, biomaterials, and semiconductors [8]. Korayem et al. have made intensive studies of the effect of capillary force on the tip-surface interactions when it is operated in air [9] and the manipulation of micro/nanoparticles on rough surfaces [10]. Furthermore, they proposed a new multiscale methodology for modeling of single and multibody to solve the multiscale dynamic problem in the nanomanipulation process [11]. Ahmadi et al. have investigated the effects of fluid environment properties on the nonlinear vibrations of AFM piezoelectric microcantilevers using a theoretical analysis [12] and FEM simulation considering tip-sample nonlinear interactions [13].

The lateral contact mode AFM is usually used to measure the mechanical properties of nanowires (NWs). In the lateral manipulation, a NW is clamped onto a flat substrate so that one end forms a cantilever. An AFM tip is moved in one direction, and the lateral force is indicated by the contact between the side of the tip and the NW. The flexural properties of NWs can be determined according to beam theory by recording the curves of contact force versus displacement ($F-\delta$ curve) [14]. By neglecting the contribution of friction force from the substrate, Wong et al. obtained the effective elastic modulus and bending strength of a NW [1]. Wang et al. derived the strain and stress of NWs from the $F-\delta$ curve [14]. Manipulation-based methods have also been used to measure the friction between a NW and a substrate, which can be calculated by counterbalancing the frictional force relative to the contact force. Xie et al. modeled the deflection of a NW as a Euler-Bernoulli beam subjected to a uniformly distributed friction and contact force [2, 3]. Hou et al. calculated

the friction of bent NWs with relatively large deformations based on force equilibrium equations [5]. Tran and Chung also obtained the elastic modulus and friction of NWs by using simple beam theory [6]. The main purpose of analyzing test results is to precisely determine the elastic bending deformation of NW.

Three factors are needed to consider when formulating the bending deformation of a NW. First, the changing position of the AFM tip along the length direction of NW implies a change in the direction of the contact force. Second, the large displacements of a slender NW subjected to a contact force imply a nonlinear relationship between the curvature and the bending moment. Third, surface effects induce additional deformation energies in NWs [15–19]. Therefore, a simple and reliable formula to calculate the flexural properties of slender NWs is necessary. In this work, we studied the effective modulus and $F - \delta$ curve of a NW on a smooth, flat substrate by using the slender Euler-Bernoulli beam model. If the NW is long enough and the distance from the tip to the fixed end of NW is not short, the contact status will retain in a certain range. The large-deflection deformation of NW implicates large rotational angle and infinitesimal strain. So this situation will be considered in our mode. The large-deflection deformation of the cantilever is formulated by surface elasticity. We then established differential and integral equations to describe the deformation via the arc differential method and bending moment balance on the cross-section of the NW. Moreover, we compared our findings with the measurement results in the literatures.

2. Model Analysis

A NW laterally manipulated by an AFM tip on a smooth, flat substrate can be modeled as a cantilever subjected to a concentrated force and a uniformly distributed friction force, as proposed in previous research. The friction force is quite small, and its contribution to the deformation of NW is negligible [1]. Figure 1 shows a schematic of a beam bending with an AFM tip. The tip moves in the vertical direction. The axial line of the beam is straight when the tip initially touches the NW (Figure 1(b)). The distance l (along the X axis) from the fixed pinning point ($X = 0$) remains constant. The position of the AFM tip changes with the bending of the NW, but the contact force remains perpendicular to the axial line of the NW (Figure 1(c)). Consequently, the contact force also changes with the deformation of the NW. Formulating the NW's bending deformation depends on the description of the position of the curved axial line. We assume that a NW AC with length L and diameter d is located in the Cartesian coordinate system OXY, where B (l, 0) is the position of the tip. The axial line can be presented as follows:

$$\begin{cases} x_0 = X + u_0(X), \\ y_0 = w_0(X), \end{cases} \tag{1}$$

where (x_0, y_0) and $(X, 0)$ are the coordinates of a point on the axial line before and after the bending deformation of the

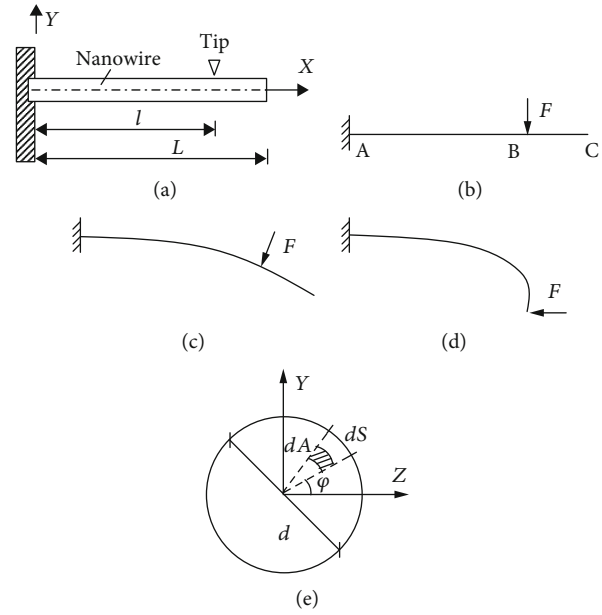

Figure 1: Schematic of the lateral manipulation. (a) A beam with a free end. (b) The initial contact between the tip and NW. (c) The bending deformation of NW. (d) The separation of the tip. (e) The cross-section of NW.

NW. u_0 and w_0 are the displacements of the axial line. The infinitesimal segment dX of the axial line can be written as

$$ds_0 = \sqrt{dx_0^2 + dy_0^2}. \tag{2}$$

Noting Equation (1), the above equation can be expressed as

$$\begin{aligned} ds_0 &= \sqrt{[dX + du_0(X)]^2 + (dw_0(X))^2} \\ &= \sqrt{\left(1 + \frac{du_0}{dX}\right)^2 + \left(\frac{dw_0}{dX}\right)^2}\, dX. \end{aligned} \tag{3}$$

The elongation ratio of segment dX is defined by

$$\Lambda_0 = \frac{ds_0}{dX} = \sqrt{\left(1 + \frac{du_0}{dX}\right)^2 + \left(\frac{dw_0}{dX}\right)^2}. \tag{4}$$

The derivatives of the displacements are

$$\begin{cases} \dfrac{du_0}{dX} = \Lambda_0 \cos\theta - 1, \\ \dfrac{dw_0}{dX} = \Lambda_0 \sin\theta, \end{cases} \tag{5}$$

where θ is the intersection angle between the tangent of the NW and the X axis (rotational angle). Hence, the strain of the axial line is

$$\varepsilon_{x0} = \frac{ds_0 - dX}{dX} = \Lambda_0 - 1. \tag{6}$$

The curvature of the axial line is

$$\kappa_0 = \frac{d\theta}{ds_0} = \frac{1}{\Lambda_0}\frac{d\theta}{dX}. \tag{7}$$

Similarly, the coordinates of a point in the beam after deformation are

$$\begin{cases} x = X + u(X, Y), \\ y = Y + w(X, Y), \end{cases} \tag{8}$$

where $Y \in [-d/2, d/2]$ and u and w are the displacements of the point. Neglecting shear deformation and applying the plane section assumptions for a beam, the displacements can be written as follows:

$$\begin{cases} u(X, Y) = u_0(X) - Y \sin\theta, \\ w(X, Y) = w_0(X) - Y(1 - \cos\theta). \end{cases} \tag{9}$$

The segment parallel to and equal to dX can be transformed into

$$ds = \sqrt{(dx)^2 + (dy)^2}. \tag{10}$$

Based on Equations (5), (8), and (9), the differential coordinates are

$$\begin{cases} dx = dX + \dfrac{\partial u}{\partial X}dX = \left(\Lambda_0 - Y\dfrac{d\theta}{dX}\right)\cos\theta dX, \\ dy = \dfrac{\partial w}{\partial X}dX = \left(\Lambda_0 - Y\dfrac{d\theta}{dX}\right)\sin\theta dX. \end{cases} \tag{11}$$

By substituting the above equations into Equation (10), the following equation can be obtained.

$$ds = \left(\Lambda_0 - Y\frac{d\theta}{dX}\right)dX. \tag{12}$$

The elongation ratio of segment dX in a beam is defined as

$$\Lambda = \frac{ds}{dX} = \Lambda_0 - Y\frac{d\theta}{dX} = \Lambda_0(1 - \kappa_0 Y). \tag{13}$$

It is found from the above equation that if $Y = 0$, $\Lambda = \Lambda_0$. Thus, Equation (13) expresses the elongation ratio of an arbitrary segment in the beam. The axial strain of the beam is

$$\varepsilon_x = \frac{ds - dX}{dX} = \Lambda - 1 = \varepsilon_{x0} - Y\Lambda_0\kappa_0. \tag{14}$$

It is found from the above equation that if $Y = 0$, $\varepsilon_x = \varepsilon_{x0}$. Thus, Equation (14) expresses the axial strain of the NW. The curvature of the NW is

$$\kappa = \frac{d\theta}{ds} = \frac{d\theta}{\Lambda dX} = \frac{\kappa_0}{1 - Y\kappa_0}. \tag{15}$$

It is also found from the above equation that if $Y = 0$, $\kappa = \kappa_0$. Thus, Equation (15) expresses the bending curvature of an arbitrary segment in the NW.

To calculate the surface energy of NW, we consider the surface strain and curvature. Adopting the polar coordinates on the cross-section of the NW shown in Figure 1(e) and substituting the relation $Y = d\sin\varphi/2$ into Equations (14) and (15), the following equations can be obtained:

$$\begin{aligned} \varepsilon_s &= (\Lambda_0 - 1) - \frac{d\Lambda_0\kappa_0}{2}\sin\varphi, \\ \kappa_s &= \frac{\kappa_0}{1 - d\kappa_0\sin\varphi/2}. \end{aligned} \tag{16}$$

Thus, the stress in the bulk material is

$$\sigma_x = E\varepsilon_x. \tag{17}$$

The surface and moment stresses are [13]

$$\tau_s = C_0\varepsilon_s, \tag{18}$$

$$m_s = C_1\kappa_s, \tag{19}$$

where C_0 is the Gurtin-Murdoch constant and C_1 is the Steigman-Ogden constant [20]. The surface stress, surface moment stress, and bulk stress balancing the bending moment, the integration over the cross-sectional area yields

$$\begin{aligned} &\iint_\Omega \sigma_x Y dA + \oint_S \tau_s Y dS + \oint_S m_s dS \\ &\quad = -[F(l - x)\cos\theta_B + P(w_{0B} - w_0)\sin\theta_B], \end{aligned} \tag{20}$$

where w_{0B} and θ_B are the deflection and rotational angle of the section on which the AFM tip acts. By substituting Equations (17), (18), and (19) into the above equation, the following equation can be obtained:

$$(EI + C_1 I^*)\frac{d\theta}{dX} = F(l - x)\cos\theta_B + F(w_{0B} - w_0)\sin\theta_B, \tag{21}$$

where $I = \iint_\Omega Y^2 dA = \pi d^4/64$ is the moment inertia of the cross-section and $I^* = \oint_S Y^2 dS = \pi d^3/8$ is the perimeter moment of inertia. The above equation provides a geometrical deformation model of a NW subjected to a contact force of the AFM tip. The flexural stiffness can be defined as $E^*I = EI + C_1 I^*$. Substituting Equation (15) into Equation (21), a nonlinear differential equation can be obtained to describe the deformation. However, this equation is difficult to solve. Thus, we adopt another method to solve this

problem. For a slender NW, we can neglect the stretch of the axial line by setting $\Lambda_0 = 1$. Taking the derived arc differential of the axial line ds_0 in Equation (21), the following equation can be obtained:

$$E^* I \frac{d^2\theta}{ds_0^2} = -F \cos(\theta_B - \theta). \tag{22}$$

By multiplying $d\theta$ to the both sides of the above equation and integrating the result, the following expression can be obtained:

$$\frac{1}{2}\left(\frac{d\theta}{ds_0}\right)^2 = \frac{F}{E^* I} \sin(\theta_B - \theta) + C, \tag{23}$$

where C is an integration constant. According to the boundary condition at the free end, $\theta = \theta_B$ and $d\theta/ds_0 = 0$; hence, $C = 0$. The arc differential is

$$ds_0 = \sqrt{\frac{E^* I}{2F}} \frac{d\theta}{\sqrt{\sin(\theta_B - \theta)}}. \tag{24}$$

The length of a NW can be expressed as

$$L = \int_0^L ds_0 = \sqrt{\frac{E^* I}{2F}} \frac{d\theta}{\sqrt{\sin(\theta_B - \theta)}}. \tag{25}$$

The distance from the fixed pinning point to the tip is

$$l = \int_0^l dx_0 = \sqrt{\frac{E^* I}{2F}} \int_0^{\theta_B} \frac{\cos\theta d\theta}{\sqrt{\sin(\theta_B - \theta)}}. \tag{26}$$

The displacement of the tip is

$$\delta = w_{0B} = \int_0^{y_{0B}} dy_0 = \sqrt{\frac{E^* I}{2F}} \int_0^{\theta_B} \frac{\sin\theta d\theta}{\sqrt{\sin(\theta_B - \theta)}}. \tag{27}$$

Equations (25) and (26) show that the right sides contain two similar terms, the ratio of flexural stiffness to contact force and the integration about the angle. Dividing Equation (26) by Equation (25), the following equation can be obtained:

$$\frac{\delta}{l} = \frac{\int_0^{\theta_B} \left(\sin\theta d\theta / \sqrt{\sin(\theta_B - \theta)}\right)}{\int_0^{\theta_B} \left(\cos\theta d\theta / \sqrt{\sin(\theta_B - \theta)}\right)}. \tag{28}$$

For a given displacement of the tip δ, θ_B can be determined from the above equation. Then, the contact force F can be calculated using Equation (26) or (27). Hence, the $F - \delta$ curve and flexural properties of the NW can be obtained.

3. Results and Discussion

The deformation of NW in lateral manipulation is influenced by the contact force and bending modulus. The surface effect of NW in manipulation is not completely discussed in the literatures. We first focus on the effect of surface elasticity of NW in lateral manipulation. According to the definition of normalized flexural stiffness, the effective modulus of NW can be expressed as $E^* = E + C_0 I^*/I$. As an example, we consider a Ag NW with a bulk-material elastic modulus of $E = 73$GPa. Molecular dynamics simulations indicate that $C_0 = -0.37938\text{eV}/\text{Å}^2$ for a $\langle 100 \rangle$ axially oriented NW and $C_0 = 2.5227\text{eV}/\text{Å}^2$ for a $\langle 110 \rangle$ axially oriented NW [20]. Figure 2 shows the normalized effective modulus (E^*/E) versus the diameter of the NW. The normalized effective modulus approaches 1 with increasing diameter. The Gurtin-Murdoch constant exerts different influences on NW, i.e., stiffening when $C_0 > 0$ and softening when $C_0 < 0$. The surface effect of NW is neglected in many models [1–6], so the total deformation energy is not calculated. Our model can give exact prediction for the effective modulus of NW. It is also found from Equations (26) and (27) that the flexural stiffness of circular NWs is independent of the Steigman-Ogden constant. The bending curvature has an antisymmetric distribution along the peripheral direction of the NW, which is different from the observed behavior in rectangular NWs. Chhapadia et al.'s formulation shows that the surface moment stress has a definite influence on the effective modulus of rectangular NWs [20]. However, the curvature-dependent elasticity of circular NWs can be neglected but for surface stress. Figure 3 shows the displacement of the AFM tip (δ/l) versus the normalized contact force ($\sqrt{2F/E^* I}$) and the rotational angle of the free end of the wire (θ_B). The nonlinear relationship between the normalized contact force and displacement is different from the linear deformation of NWs with small deflections. The interaction between the AFM tip and NW can be divided into two stages. The first stage shows an increase in contact force with increasing displacement. The normalized contact force reaches a maximum value of 2.357 when $\delta/l = 0.7218$. The second stage shows a decrease in contact force until the tip's separation when the normalized contact force is 1.44. We also determine the nonlinear relationship between the rotational angle and displacement. At $\theta_B = 54°$, the contact force reaches a maximum value. At $\theta_B = 90°$ and $\delta/l = 1.67$, the tip leaves the NW, which implies

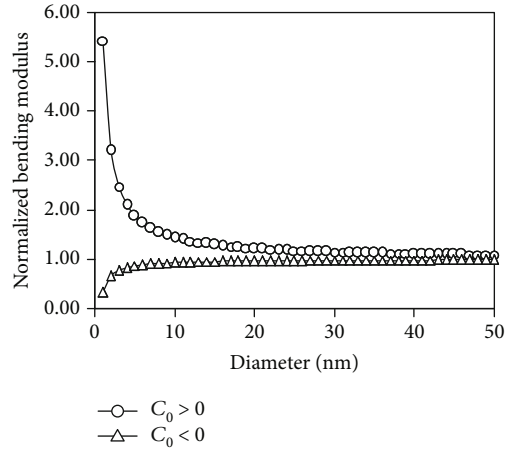

Figure 2: The normalized effective the NW.

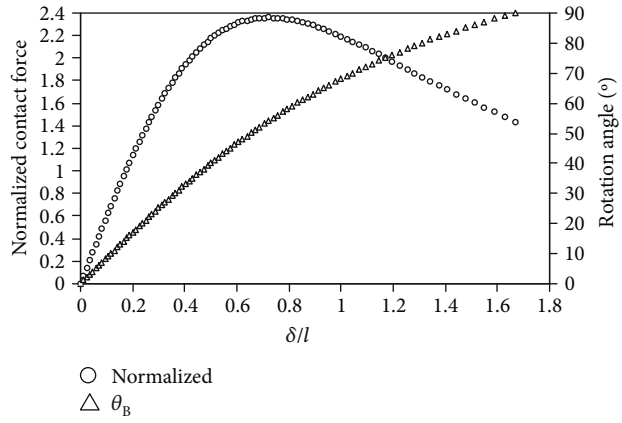

Figure 3: The normalized contact force and rotation angle of NW.

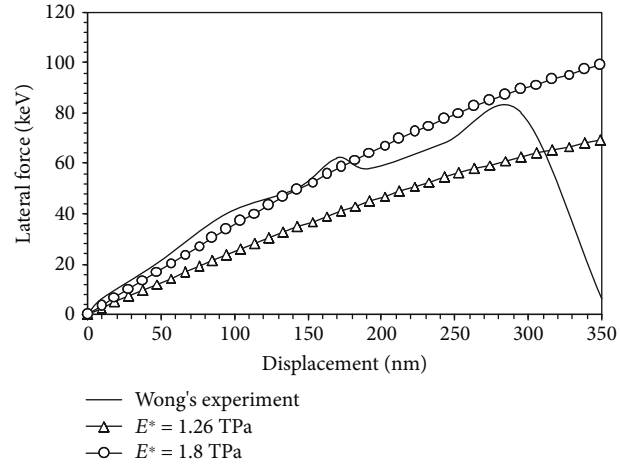

Figure 4: The lateral force vs. the displacement of the tip.

that the minimum length of the NW is 2.19 times the distance from the fixed pinning point and then retain the contact status between the tip and the NW.

Special attention is devoted to the degree of deformation of NW in lateral manipulation. Wong et al.'s measurement of multiwall carbon nanotubes with a diameter of 32.9 nm and length of 1 μm showed that the effective elastic modulus of the tubes is 1.26 TPa, the bending deflection is approximately 170 nm, and the rotational angle is approximately 10° at $l = 813$nm [1]. The deflection observed is 4.86 times the diameter and 0.2 times the length and, thus, can be classified as a large displacement problem. Simple beam theory predicts $\theta_B = Fl^2/2E^*I$, $\delta_B = Fl^2(3L - l)/6E^*I$; thus, the predicted δ_B/θ_B is approximately 12.717nm/°, which is smaller than the measured amount of 170nm/10°. Using our model and according to Equation (28), $\delta_B/l = 0.21$, the predicted rotational angle is approximately 18°. The prediction is in a good accordance with the measurements. Figure 4 compares our predictions with Wong et al.'s experimental results. The $F - \delta$ curve with $E^* = 1.26$TPa is located under Wong et al.'s curve, which implies that the theoretical flexibility is larger than its experimental counterpart. Hence, simple beam theory will underestimate the deformation of NW in manipulation. We found that the predicted $F - \delta$ curve, which assumes an effective elastic modulus of 1.8 TPa, matches Wong et al.'s results well. Considering the change in load position and direction of the AFM tip, simple beam theory cannot provide the exact bending moment and axial profile of the NW. For a slender NW, the estimated effective elastic modulus based on simple beam theory during manipulation is smaller than the actual measurement. We therefore propose considering the deformation of NWs as a large displacement problem.

We further focus on the influence of contact force on the bending deflection of NW in lateral manipulation. In much manipulations to measure the friction characteristics of NW, the AFM tip was placed near the free end of the NW so that $l \in [0.9L, L)$ [6]. In this case, however, separation of the tip will occur, and the free end of NW could deform via a small rotational angle. Our calculations show that the rotational angle varies from 0° – 35°, which is much smaller than the angle ($\theta_B = 57°$) of long NWs. The deformation of NWs during manipulation corresponds to the linear range in the first stage (Figure 3). In this range, the normalized contact force ranges from 0 to 2.02, and δ/l varies from 0 to 0.43. Tran and Chung's lateral manipulation experiment involving SiO NWs with a diameter of 140 nm and length of 1.84 μm showed that the maximum bending deflection of the NW is 430 nm and its effective elastic modulus is 84 ± 7GPa [6]. This deflection is approximately 3 times the diameter and 0.23 times the length. Hence, simple beam theory cannot provide an approximate description of the large displacement of NWs. According to Equation (27), $\delta_B/l = 0.23$, and the predicted rotational angle is approximately 28°, which is a considerable amount compared with the assumption of infinitesimal rotation in simple beam theory. The predicted contact force is approximately 0.192 μN, which is much smaller than the experimental value obtained. This observation could be attributed to friction. Considering that friction is neglected in our model, the deflection of NW may be amplified. However, the distribution of friction can be considered to be perpendicular to the deformed axial curve of the NW, which can also be described by a large displacement and large rotational angle problem.

In a conclusion, surface stress and contact status are the two key points of prediction for the flexural properties of slender NWs in lateral manipulation. However, the surface stress is not taken into account in many studies. The size effects have been formulated by curvature-dependence surface elasticity. We found that the surface stress would increase or decrease the flexural stiffness of circular NWs. For the shape of noncircular cross-section, the influence of surface curvature is also needed to investigate. Furthermore, the degree of deformation determines the scope of simple beam theory for the lateral manipulation application when the tip leaves the NW. In many manipulations, NWs present large deflection and large rotation. Our model gives a detailed large deflection formulation of a slender NW in the whole manipulation process. The predictions for the effective elastic modulus, deflection, and rotation of NW are in accordance with the measurements in the literature. It is noted that the friction and shear on the cross-section are not considered due to the smooth substrate. The contribution of the constant

friction to the bending moment still can be calculated by Equation (21). Moreover, we only establish the balance on the bending moment, so the influence of shear is neglected for a slender NW (which is different from Timoshenko beam). The readers are referred to the work of Haefner and Willam [21] for the large deflection formulations of a simple beam including shear deformations.

4. Conclusions

In this work, we described the geometry of a beam axial line using integral equations to improve the description of the large-deflection deformation of NWs during lateral manipulation. The $F - \delta$ curve and rotational angle of NWs can be directly determined by solving these integral equations to avoid the necessity of solving complex nonlinear differential equations. The proposed approach can readily explain all of the flexural properties of NWs, such as their effective modulus and stiffness. Whereas surface moment stresses have no effect, surface stresses have a definite influence on the effective modulus of circular NWs. A positive Gurtin-Murdoch constant has a stiffening effect on NWs, while a negative constant has a softening effect. The $F - \delta$ curve obtained is different from that predicted by using simple beam theory, which is usually adopted in lateral manipulation. The contact force does not increase with increasing displacement, and the $F - \delta$ curve exists a maximum amount due to the change in load position and direction of the AFM tip. Therefore, the use of simple beam theory during manipulation will underestimate the deflection and effective modulus of NWs. Our model highlights the importance of the geometry of the axial profile of NWs. The predicted $F - \delta$ curve and rotational angle may match the experimental results well by ensuring the appropriate amplification of the effective modulus of NWs. We confirm that the distribution of friction could be described by large displacement and rotational angle problem during measurement of the friction characteristics of NWs.

Data Availability

The cited experimental data used to support the findings of this study are included within the article.

Conflicts of Interest

The authors declare that they have no conflicts of interest.

Acknowledgments

The authors gratefully acknowledge the financial supports to this work from the National Engineering Laboratory for Highway Tunnel Construction Technology (Grant No. NELFHT201702) and the Key Research Project of Xihua University (Grant No. z1320608).

References

[1] E. W. Wong, P. E. Sheehan, and C. M. Lieber, "Nanobeam mechanics: elasticity, strength, and toughness of nanorods and nanotubes," *Science*, vol. 277, no. 5334, pp. 1971–1975, 1997.

[2] H. Xie, S. Wang, and H. Huang, "Characterising the nanoscale kinetic friction using force-equilibrium and energy-conservation models with optical manipulation," *Nanotechnology*, vol. 27, no. 6, pp. 065709–065716, 2016.

[3] H. Xie, S. Wang, and H. Huang, "Kinetic and static friction between alumina nanowires and a Si substrate characterized using a bending manipulation method," *Journal of Materials Research*, vol. 30, no. 11, pp. 1852–1860, 2015.

[4] S. Wang, L. Hou, H. Xie, and H. Huang, "The kinetic friction between a nanowire and a flat substrate measured using nanomanipulation with optical microscopy," *Applied Physics Letters*, vol. 107, no. 10, 2015.

[5] L. Hou, S. Wang, and H. Huang, "A simple criterion for determining the static friction force between nanowires and flat substrates using the most-bent-state method," *Nanotechnology*, vol. 26, no. 16, pp. 165702–165708, 2015.

[6] D. K. Tran and K. H. Chung, "Simultaneous measurement of elastic properties and friction characteristics of nanowires using atomic force microscopy," *Experimental Mechanics*, vol. 55, no. 5, pp. 903–915, 2015.

[7] B. Bhushan, *Springer Handbook of Nanotechnology*, Springer, Berlin, Heidelberg, 3rd edition, 2010.

[8] M. H. Korayem, A. Kavousi, and N. Ebrahimi, "Dynamic analysis of tapping-mode AFM considering capillary force interactions," *Scientia Iranica*, vol. 18, no. 1, pp. 121–129, 2011.

[9] M. H. Korayem and E. Omidi, "Robust controlled manipulation of nanoparticles using atomic force microscope," *Micro & Nano Letters*, vol. 7, no. 9, pp. 927–931, 2012.

[10] M. H. Korayem and M. Zakeri, "Dynamic modeling of manipulation of micro/nanoparticles on rough surfaces," *Applied Surface Science*, vol. 257, no. 15, pp. 6503–6513, 2011.

[11] M. H. Korayem, S. Sadeghzadeh, and V. Rahneshin, "A new multiscale methodology for modeling of single and multibody solid structures," *Computational Materials Science*, vol. 63, pp. 1–11, 2012.

[12] M. Ahmadi, R. Ansari, and M. Darvizeh, "Free and forced vibrations of atomic force microscope piezoelectric cantilevers considering tip-sample nonlinear interactions," *Thin-Walled Structures*, vol. 145, article 106382, 2019.

[13] M. Ahmadi, R. Ansari, M. Darvizeh, and H. Rouhi, "Effects of fluid environment properties on the nonlinear vibrations of AFM piezoelectric microcantilevers," *Journal of Ultrafine Grained and Nanostructured Materials*, vol. 50, no. 2, pp. 117–123, 2017.

[14] S. Wang, Z. Shan, and H. Huang, "The mechanical properties of nanowires," *Advanced Science*, vol. 4, no. 4, 2017.

[15] C. Q. Chen, Y. Shi, Y. S. Zhang, J. Zhu, and Y. J. Yan, "Size dependence of Young's modulus in ZnO nanowires," *Physical Review Letters*, vol. 96, no. 7, 2006.

[16] M. E. Gurtin and A. I. Murdoch, "A continuum theory of elastic material surfaces," *Archive for Rational Mechanics and Analysis*, vol. 57, no. 4, pp. 291–323, 1975.

[17] R. E. Miller and V. B. Shenoy, "Size-dependent elastic properties of nano-sized structural elements," *Nanotechnology*, vol. 11, no. 3, pp. 139–147, 2000.

[18] F. Xu, Q. Qin, A. Mishra, Y. Gu, and Y. Zhu, "Mechanical properties of ZnO nanowires under different loading modes," *Nano Research*, vol. 3, no. 4, pp. 271–280, 2010.

[19] D. J. Steigmann and R. W. Ogden, "Elastic surface substrate interactions," *Proceedings of the Royal Society of London A*, vol. 455, no. 1982, pp. 437–474, 1999.

[20] P. Chhapadia, P. Mohammadi, and P. Sharma, "Curvature-dependent surface energy and implications for nanostructures," *Journal of the Mechanics and Physics of Solids*, vol. 59, no. 10, pp. 2103–2115, 2011.

[21] L. Haefner and K. J. Willam, "Large deflection formulations of a simple beam element including shear deformations," *Engineering Computations*, vol. 1, no. 4, pp. 359–368, 1984.